Artificial Neural Network Prediction for Thermal Characteristics of Nanofluid over a Stretching Sheet with Variable Properties

Saman Iftikhar[1], Atifa Latif[2], Taha Azam[2], Ayesha Bibi[2]
[1]Faculty of Computer Studies, Arab Open university, Saudi Arabia
[2]Department of Mathematics, GC University Faisalabad Pakistan,
*Correspondence: aatifalatif@gmail.com

Citation | Iftikhar. S, Latif. A, Azam. T, Bibi. A, "Artificial Neural Network Prediction for Thermal Characteristics of Nanofluid over a Stretching Sheet with Variable Properties", IJIST, Vol. 8 Issue. 10 pp 4012-4029, November 2026
Received | Sep 20, 2026 **Revised |** Oct 25, 2026 **Accepted |** Oct 28, 2026 **Published |** Nov 02, 2026.

Stagnation-point heat transmission is one such crucial phenomenon taking place in various industrial and technical processes, particularly those involving stretched surfaces. In this study the heat transfer qualities of nanofluids flow towards a stretched sheet under boundary conditions at stagnation point with variable thermophysical properties have been investigated using an ANN framework. Compared to conventional fluids, nanofluids which consist of a base fluid and suspended nanoparticles perform better in heat transmission and have a higher thermal conductivity. The mathematical model in the form of governing partial differential equations has been obtained and transformed into nonlinear ordinary differential equations using the appropriate similarity transformations. These differential equations have subsequently been solved using the appropriate numerical techniques in BVP4c solver in MATLAB. In order to describe and forecast the heat transfer behavior of nanofluids close to a stretching sheet with variable thermophysical properties, the current study explores the use of Artificial Neural Networks (ANN) in physical problems. The impact of important parameters such as the stretching parameter, Prandtl number, nanoparticle volume fraction, and variable property parameters on the velocity and temperature profiles is examined. The ANN model has been trained using the numerical solutions obtained from MATLAB BVP4c. It was observed that the heat transfer performance improves by increasing the nanoparticle concentration. The numerical findings have compared the trained network predicts velocity profile, temperature field and concentration with minimum inaccuracy. The work demonstrates improvements in thermal systems that incorporate nanofluids on stretched surfaces with potential utilizations in cooling technologies.

Keywords: Bvp4c Approach; Artificial Neural Network; Levenberg Marquardt Technique with Back Propagations; Nano Fluid; Heat Transfer; Variable Flow Properties; Stretching Sheet, Stagnation Point.

Nomenclature:			
T	Temperature(k)	u, v	Velocity components
∞	Free Steam	ν	Kinematic viscosity
f	Rescaled nanoparticles volume fraction, nanoparticle concentration	w	sheet, wall, surface
D_B	Brownian diffusion coefficient	$Drift-flux$	The drift flux model
N_t	Thermophoresis Parameter	D_T	Thermophoresis diffusion coefficient
N_b	Brownian motion parameter	Nu	Nusselt number
Re_x	Local Reynold number	ϕ	Nanoparticle volume friction
(ρC)	Heat capacity $\frac{j}{m^3 k}$	α	thermal diffusivity $\frac{m^2}{s}$
μ_{nf}	Nanofluid viscosity	ρ_{nf}	Nanofluid density
k	thermal conductivity $\frac{w}{mk}$	Pr	Prandtl number
ρ	Density $\frac{kg}{m^3}$	N_c	Variable thermal conductivity parameter
N_v	Variable viscosity parameter	bf	The base fluid
h	Convective thermal transmission variable $\frac{j}{m^2}$	φ	nanoparticle volume fraction
np	Nanoparticle	k_f	Fluid thermal conductivity
NFs	Nanofluids	P	Pressure (Pa)
Le	Lewis number	η	Dimensionless distance
C_p	Specific heat capacity	q_m	Mass heat flux
q_w	Surface heat flux	τ_w	Surface shear stress
θ	Dimensionless temperature	ψ	Stream function
μ	Viscosity (Pa s)	ν	Kinematic viscosity
Abbreviations.			
Ar.E	Arrhenius Equations	BPLMT	Back propagation by Levenberg Marquart Technique
R.As	Regression analysis	ANNs	Artificial Neural Networks
AI	Artificial intelligence	BNF	Buongiorno nanofluid
ANN-GA	Artificial neural network genetic algorithm	Er.H.As	Error histogram analysis
NN	Neural Network	AE	Absolute error
SQP	Sequential quadratic programming	MSE	Mean squared error

Introduction:

Heat transfer in nanofluids flowing across a stretching sheet with variable characteristics is modelled and predicted using the Artificial Neural Network technique. This method is effective for understanding behaviors and gives reliable results. Nanofluids are kinds

of fluids that prepared by adding nanoparticles such as coper, gold, silver, titanium and aluminum ect to liquids like water, oil and glycerin etc. [1] investigated the magnetohydrodynamic (MHD) stagnation point flow of nanofluids over a stretching surface with variable thickness under the influence of thermal radiation. Their study analyzed that magnetic fields and surface geometry affect heat transfer characteristics significantly. [2] investigated the flow and thermal transformation of nanofluids nearer the stationary region beyond a permeable nonlinear stretched cylinder and the analysis focused on the effects of suction or injection and nonlinear stretching parameters on velocity & temperature profiles. [3] studied nanofluid stagnation point flow toward a stretching sheet in a porous medium with heat generation and reported an improvement in the heat transfer rate in the presence of nanoparticles. Additionally, [4] investigated nanofluid flow by considering electromagnetic effects, radiation, and variable heat flow. [5] offered a comparable solution that included heat generation and absorption as well as suction and blowing effects for boundary layer's stationary points flowing in the direction of a nanofluid-saturated thermally permeable stretched surface. [6] discovered that the morphology of ZnO nanoparticles has a significant impact on the parameters of nanofluids. [7] improved convectional temperature flow and heat conductance while marginally increasing viscosity, according to a scientific investigation of MgO–H2O nanofluids under turbulent flow.

Artificial neural networks have gained much popularity in modern age as a powerful tool for complex mathematical modeling of highly nonlinear systems for the prediction of physical problems. In the context, [8][9][10] created an artificial neural network model based on the heat and mass transfer in dissipative Williamson fluid, Buongiorno model and viscoelastic fluidic flow respectively to examine nanofluid flow over a stretching sheet. They applied Cattaneo-Christov heat and mass transfer as well as Fourier methods for their problems using intelligent prediction networks. The study showed that the prediction by neural networks can improve computing efficiency in nanofluid simulations by properly predicting heat and mass transfer characteristics.

Mathworks developed MATLAB, a programming language and computing environment that people use to do math and science work. MATLAB is widely used in engineering and applied mathematics and also in mechanics and heat transfer research. Many researchers use MATLAB to solve differential equations that come from simplifying partial differential equations. [11] Recent advancements also include the study of carbon nanotube-based nanofluids along flexible dispersion and convection boundaries circumstances, showing enhanced instances of thermal energy and mass transmission. [12] utilized the MATLAB BVP4C technique to study nanofluid flow across a transient stretched surface, incorporating thermophores and Brownian motions implication. They found that both mechanisms enhance temperature and concentration profiles, improving overall heat transfer performance. [13] examined the stagnation-point heat transmission of nanofluids across stretching sheets while taking into account different thermophysical characteristics. Their findings showed that velocity and temperature distributions are strongly affected by changes in properties. Abd El- [14] analyzed stagnation-point flow over a porous stretching sheet using similarity transformations. Further studies explored the implication of chemically reacted and unsteady flow conditions on heat transfer characteristics. [15] The role of variable viscosity and radiative heat transfer in nanofluid flow was also emphasized to better represent practical scenarios. [16]Subsequent research expanded the understanding of stagnation-point flow by incorporating more complex fluid models and physical phenomena. [17] while non-Newtonian fluid models such as Williamson fluids were studied under unsteady conditions with additional effects like Ohmic heating.

The results showed that Artificial Neural Network (ANN) models greatly reduce the cost of computation and provide predictions compared with conventional numerical methods.

The study found that machine learning algorithms can accurately guess fluid flow and heat transfer behavior. ANN models can accurately predict problems. [18] Moreover, temperature-dependent viscosity has been identified as a critical factor in accurately predicting boundary layer behavior and thermal performance in practical engineering systems. [19] To replicate actual biological and environmental systems, more intricate phenomena like thermo-bioconvection and the existence of motile microorganisms have also been included. [20] Analytical models have been validated and oblique stagnation-point flows have been analyzed using numerical approaches, such as finite difference methods. [21] Pantograph delay differential equations were solved using Levenberg-Marquardt and Bayesian regularization backpropagation neural networks.

The ANN model usually enhances computing efficiency while properly predicting flow and thermal characteristics in fluidic problems. [23] created a numerical–ANN framework to use the Bvp4c approach to evaluate MHD water-dependent Prandtl nanofluids flowing across a stretched cavity. According to the study, the ANN model lowered computational complexity and accurately predicted heat and flow behavior. [24] modeled and optimized the effective parameters influencing nanofluid change in heat performance by combining artificial neural networks with genetic algorithms. [25] created a well-trained artificial neural network (ANN) using the Levenberg–Marquardt algorithm. [26] investigated Maxwell nanofluid flow across a stretching sheet with chemical reaction and heat radiation effects using a Bayesian regularization Artificial Neural Network (BRANN). According to their findings, the ANN model minimized computational error while producing extremely accurate predictions for nonlinear heat and fluid flow behavior. [27] examined the use of Artificial Neural Networks (ANN) to analyze ternary hybrid nanofluids movement along a stretched surface. The results showed that Artificial Neural Network (ANN) models greatly reduce the cost of computation and give answers when compared to old numerical methods.

The novelty of present work is to investigate the dominant effects of chemical reaction and viscous dissipation on boundary layer stagnation point flow across a stretched sheet in a nanofluid with uniform wall temperature, concentration and nanoparticle concentration. The ANN-BPLMT approach based on Levenberg–Marquardt back propagation is used in the present work to forecast the given model utilizing BVP4c-generated solutions of the transformed ODEs as the reference dataset for MATLAB-based neural network training and evaluation.

Rest parts of the presented study is organized as follows: Section 2 is prepared for Mathematical Modeling for the Buongiorno nano-fluid flow, Section 3 is constructed for Solution Methodology for physical problem, Section 4 depicts the Results and Discussion, Solution and Error plots are given in Section 5 whereas the last Section contains the Conclusion of the study.

Mathematical Model of BNFs:

The following points summarize the two-dimensional convective flow past a stretched sheet.

- The analysis focuses on the flow along a plane, $y = 0$, and stagnation point, $x = 0$, are taken into consideration, passes across a stretched sheet in the area $y > 0$.
- It is assumed that the flow is laminar, consistent, and incompressible.
- Consider heat transfer and 2-dimensional incompressible stagnation-point flow of a nanofluid across a porous, isothermal stretched horizontal sheet.
- A geometry (Fig. 1) illustrating the flow behavior close to the stretching surface serves as a representation of the physical model.
- The Buongiorno model states that thermophoresis and Brownian diffusion are the two fundamental factors influencing nanoparticle movement.

- Nanoparticles migrate across the heated surfaces to the cooler fluid's region as a consequence of thermophoresis.
- A more homogeneous distribution of nanoparticles is produced via Brownian motion, which drives particles from areas of higher concentration to areas of lower concentration.
- It is assumed that the nanofluid is a diluted combination with a volume fraction of less than 3% of nanoparticles.
- It is assumed that the base fluid and nanoparticles are in local thermal equilibrium.
- The consequences of chemical reactions and heat production inside the boundary layer are disregarded.
- The nanofluids dynamic viscosity and thermal conductivity change linearly with the volume percentage of nanoparticles.
- The governing equations for continuity, momentum, energy, and concentration are made simpler by using boundary layer approximations.

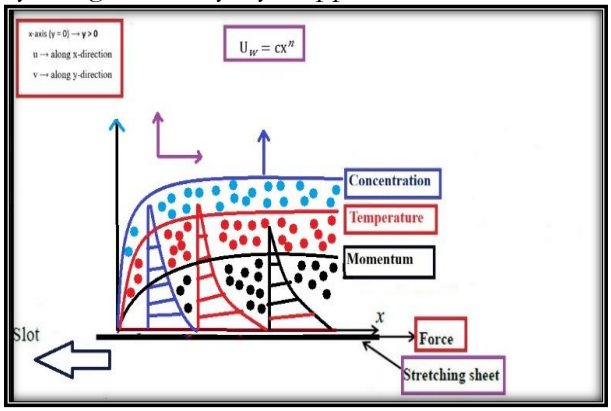


Figure 1. A graphic illustration of the problem

The governing equations for stretching sheets with $a > 0$ are as follows:

$$\frac{\partial u}{\partial x}+\frac{\partial v}{\partial y}=0, \tag{1}$$

$$\rho_{nf}\left(u\frac{\partial u}{\partial x}+v\frac{\partial u}{\partial y}\right)=-\frac{\partial p}{\partial x}+\frac{\partial}{\partial x}\left(\mu_{nf,\infty}\frac{\partial u}{\partial x}\right)+\frac{\partial}{\partial y}\left(\mu_{nf,\infty}\frac{\partial u}{\partial y}\right).$$

$$\rho_{nf}\left(u\frac{\partial v}{\partial x}+v\frac{\partial v}{\partial x}\right)=-\frac{\partial p}{\partial y}+\frac{\partial}{\partial x}\left(\mu_{nf,\infty}\frac{\partial v}{\partial x}\right)+\frac{\partial}{\partial y}\left(\mu_{nf,\infty}\frac{\partial v}{\partial y}\right). \tag{2}$$

$$u\frac{\partial T}{\partial x}+v\frac{\partial T}{\partial y}=\frac{1}{(\rho c)_{nf}}\left[\frac{\partial}{\partial x}\left(\kappa_{nf,\infty}\frac{\partial T}{\partial x}\right)+\frac{\partial}{\partial y}\left(\kappa_{nf,\infty}\frac{\partial T}{\partial y}\right)\right]$$
$$+\tau\left[D_B\left(\frac{\partial\varphi}{\partial x}\frac{\partial T}{\partial x}+\frac{\partial\varphi}{\partial y}\frac{\partial T}{\partial y}\right)+\frac{D_T}{T_\infty}\left[\left(\frac{\partial T}{\partial x}\right)^2+\left(\frac{\partial T}{\partial y}\right)^2\right]\right]. \tag{3}$$

$$u\frac{\partial\varphi}{\partial x}+v\frac{\partial\varphi}{\partial y}=\left(\frac{\partial^2\varphi}{\partial x^2}+\frac{\partial^2\varphi}{\partial y^2}\right)D_B+\frac{D_T}{T}\left(\frac{\partial^2 T}{\partial x^2}+\frac{\partial^2 T}{\partial y^2}\right). \tag{4}$$

Boundary conditions

$$\left.\begin{aligned} u = u_w(x) = cx, \qquad & v = 0, \\ T = T_w, \qquad \frac{\partial \varphi}{\partial y} D_B + \frac{D_T}{T_\infty} = 0 \qquad & at \;\; y=0 \\ u \to u_e(x) = ax, \qquad & v \to 0, \\ T \to T_\infty, \quad \varphi \to \varphi_\infty \qquad & as \; y \to \infty. \end{aligned}\right\}. \tag{5}$$

To convert the PDEs above into nonlinear ODEs, consider the following similarity variables:

$$\eta = \frac{y}{x} R_{e_x}^{\frac{1}{2}}, \qquad S = \frac{\psi}{(U_{nf,\infty} V_{nf,\infty} x)^{\frac{1}{2}}},$$

$$\theta = \frac{T - T_\infty}{T_W - T_\infty}, \qquad \text{and} \qquad f = \frac{\phi - \phi_\infty}{\phi_\infty}.$$

By using these similarity variables in equations 1 to 5 yielded the following non dimensional system:

$$(\frac{\mu_{nf}(f)}{\mu_{nf,\infty}}) S''' + (\frac{\mu_{nf}(f)}{\mu_{nf,\infty}})' S'' + \frac{1}{2} S S'' + 1 = 0. \tag{6}$$

$$(\frac{k_{nf}(f)}{k_{nf,\infty}}) \theta'' + (\frac{k_{nf}(f)}{k_{nf,\infty}})' \theta' + \frac{1}{2} \Pr_{nf} S\theta' + N_b f'\theta' + N_t \theta'^2 = 0. \tag{7}$$

$$f'' \frac{1}{2} L_e S f' + \frac{N_t}{N_b} \theta'' = 0. \tag{8}$$

Hence boundary conditions are

$$\left.\begin{aligned} s(0) = 0, \; s'(0) = \frac{c}{a}, \; \theta(0)=1, \\ N_b f'(0) + N_t \theta'(0) = 0, \\ S'(\infty) \to 1, \; \theta(\infty) \to 0, \; f(\infty) \to 0, \end{aligned}\right\}. \tag{9}$$

Eqs. (6–8) subject to the boundary conditions given in Eq. (9) represent the resulting nondimensional differential equations and have subsequently been solved using the appropriate numerical techniques in MATLAB's BVP4c solver. The numerical methods such as Range-Kutta and Collocation techniques are built-in methods of bvp4c through MATLAB. The graphical results on these numerical values are also demonstrated below (Figure 2) for velocity, temperature and concentration with discussions.

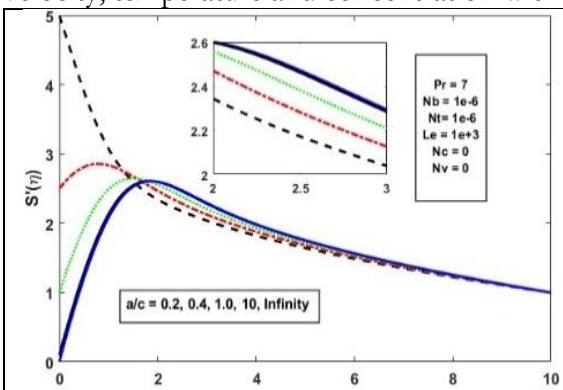


Figure. a) The impact of a/c on velocity boundary layer.

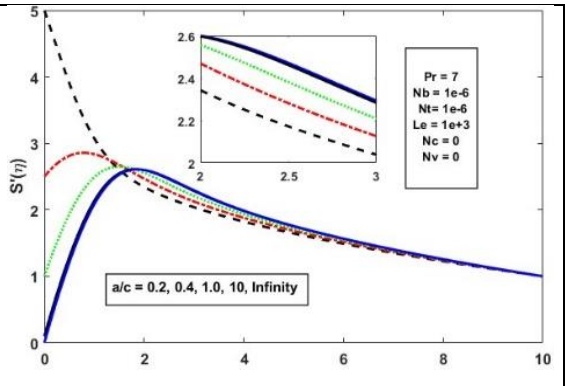


Figure. b) The impact of a/c on thermal boundary layer.

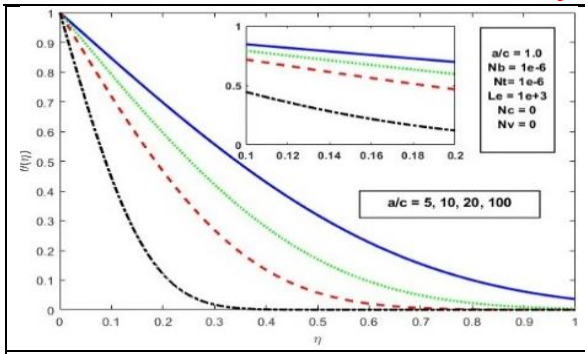


Figure. c) The impact of Prandtl numbers on thermal boundary layer.

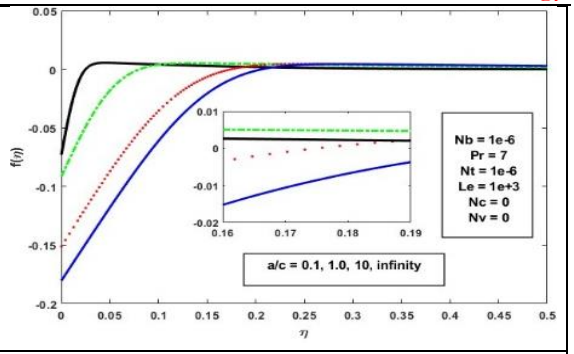


Figure. d) The impact of a/c on concentration boundary layer.

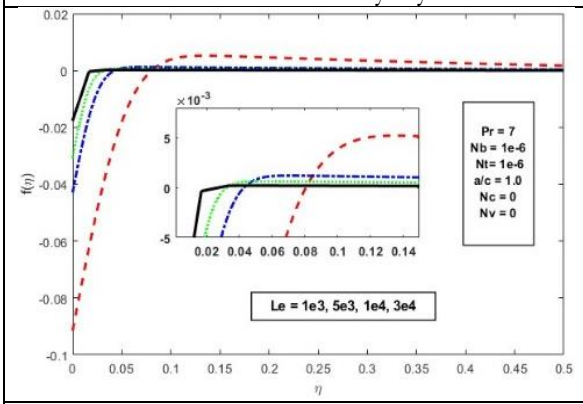


Figure. e) The impact of Lewis number on concentration boundary layer.

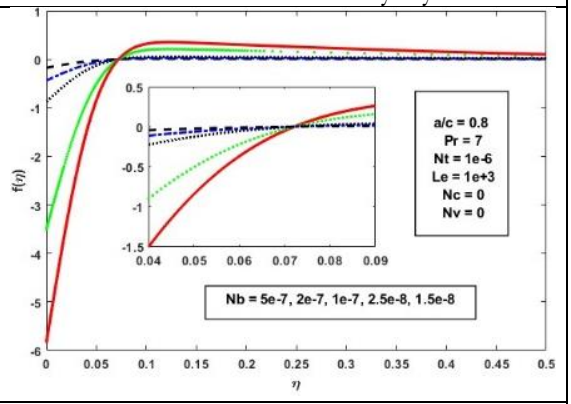


Figure. f) The impact of Brownian motion on concentration boundary layer.

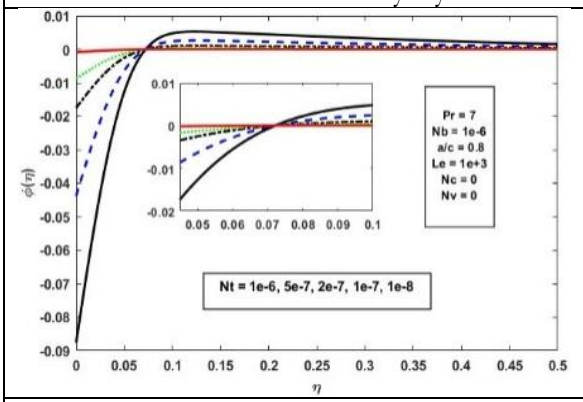


Figure. g) The impact of thermophoresis parameter on concentration.

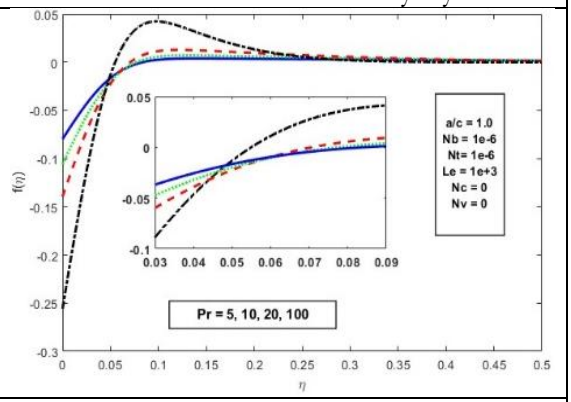


Figure. h) The impact of Prandtl numbers on concentration.

Figure 2. Impact of emerging parameters on all profiles

Implication of the stretching ratio parameter (a/c) on the entropy generation $S^{'}(\eta)$ can be seen in Figure a). Clearly by enhancing the (a/c) value, the entropy generations along the boundary layers decreases where the low value of (a/c) causes greater entropy generation because of higher velocity intensity and a stronger temperature gradient near the stretching surface to the stretching surface. From the figure also notice that At the initial stage, entropy production increases up to a certain point after which slowly decreased with η (similarity variable). In addition to this at far distance from surface all profiles converged that shows no effect on a/c parameter here. Finally, it can be concluded that stretching ratio parameters play a significant role to control the thermal irreversibility in flow.

Figure b) shows the effect of the stretching ratio parameter (a/c) on the temperature profile $\theta'(\eta)$. We observe that by increasing a/c, there occurs a decrease in the temperature distribution over the whole boundary layer. A physical explanation can be given for this phenomenon. An enhance in the value of the stretching ratio enhances the rate of heat transfer from the surface to surrounding. This causes a thinning in the thermal boundary layer which causes the fluid to cool more rapidly with increase in the value of stretching ratio.

The impact of the stretching ratio parameter (a/c) upon the temperature profile $\theta(\eta)$ has been demonstrated through Figure c). It can be noticed that an increase in a/c results in a decrease in the value of temperature as well as reduction in the magnitude of thermal boundary layer thickness. This happens due to strengthening in convection by enhancing the rate of heat transfer at high stretch rates from the sheet. As expected, temperature profiles show continuous decrease for increased values of a/c.

As shown in Figure d), improving the stretching ratio parameter (a/c) causes suppression of the concentration profile $f(\eta)$ at the vicinity of the stretching surface. Physically this can be explained by enhanced mass transport due to higher degree of stretching which diminishes nanoparticle accumulation inside boundary layer, resulting in lower thickness of nanoparticle concentration boundary layer for increased values of a/c.

Effect of Lewis number on concentration profile (Nb) can be seen from Figure e). It has been noticed that with increase in Lewis number (Le), there will be decrease in concentration boundary layer thickness. Physically this implies that greater Lewis numbers (Le) correspond to smaller Brownian diffusivity thereby limiting the movement of nanoparticles inside the liquid. This causes faster decay of concentrations distributions for large outcomes of (Le).

The impact of the Brownian motions component (Nb) on the concentration profile $f(\eta)$ is illustrated through Figure f) It can be noticed from this figure that an increase in has (Nb) a significant enhancement effect on the concentration profiles all over the boundary layer. Physically speaking, an increase in Brownian motion will cause the higher random movement of nanoparticles which eventually leads to better dispersion of the particles inside the fluid flow, thus producing a thickened concentration boundary layer with an increment in the value of (Nb).

Effect of the thermophoresis parameter (Nt) on the concentration profile $f(\eta)$ is given in Figure g). It can be seen that when we increase the value of (Nt) , then the nanoparticle concentration in the boundary layer increases. Physically, this happens because more intense thermophoretic force pulls down the nanoparticles from the hot surface into the colder portion of the fluid where their accumulation rate increases consequently causing an increment in the concentration boundary layer thickness for larger effects of (Nt).

The effect of the Prandtl number (Pr) on the concentration profile $f(\eta)$ has been displayed through Figure h). We can observe from this figure that an increase in the Prandtl number decreases the concentration profile resulting into thinning of the concentration boundary layer. This happens because high value of (Pr) means low thermal diffusivity and therefore transport of nanoparticles becomes weaker due to higher values of (Pr) , making them decay faster.

Solution methodology for ANN:

To enhance computational efficiency and predictive capability, an ANN model is developed to approximate the nonlinear behavior of the unsteady nanofluid system. Although the numerical solutions obtained using the BVP4C solver are accurate, repeated simulations

for different values of governing parameters increase computational time. Therefore, the ANN is employed as an efficient surrogate modeling technique to learn the relationship between the physical parameters and the corresponding velocity and temperature distributions within the boundary layer.

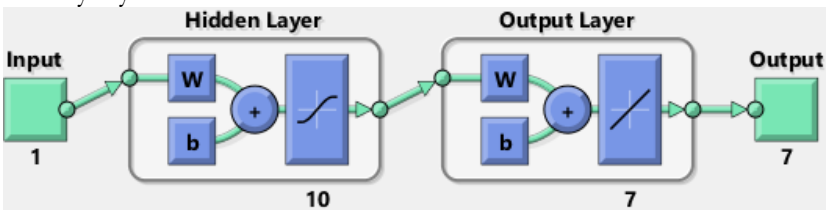


Figure 3. Neuro Structure of BNF-BPLMT

The ANN is designed as a feedforward neural network consisting of three main layers, as shown in Figure 3.

Input layer

Hidden layer

Output layer

The input layer receives the independent variables and governing parameters, including the similarity variable η, stretching parameter S , radiation parameter Rd, β suction parameter λ , Prandtl number $\Pr$, and porosity parameter. These parameters represent the physical features of the flow problem. The similarity variable η defines the spatial coordinate in transformed form and characterizes the translation effects. The radiation parameter Rd accounts for radiative heat transfer influence, the Prandtl number $\Pr$ represents the ratio of momentum diffusivity to thermal diffusivity, and the stretching parameter S describes the rate of surface stretching. The suction parameter λ and porosity parameter k further influence the boundary layer behavior. Together, these inputs define the thermofluidic state of the nanofluid.

The hidden layer processes the input signals through weighted connections and bias terms. Each neuron processes the received inputs mathematically and It then applies an activation function to produce an output. In this project we use a rule called the tangent sigmoid rule, which is really good at finding complicated connections between the things we put in and the things we get out. This special rule helps the network to understand the nonlinear relationships between the energy and momentum equations.

The output layer gives us the following values of:

- Velocity profile that is $f'(\eta)$
- Temperature profile that is $\theta(\eta)$.

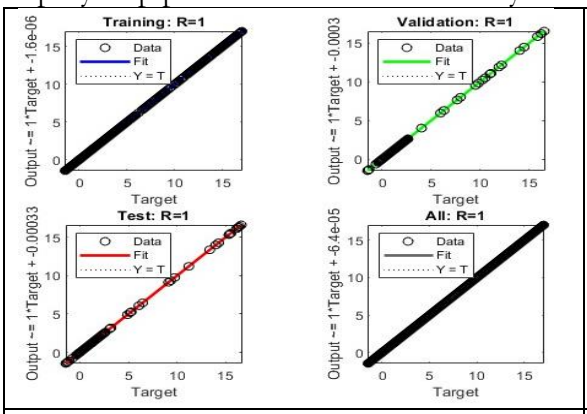
A linear activation function is used in the output layer to ensure continuous and smooth predictions of the physical quantities. After obtaining a bank of data given in table 1, the Artificial Neural Network model is trained to predict the flow characteristics. The heat is distributed for new results without having to solve the complicated math problems again. This saves a lot of computer time while still matching the solution very closely which makes the Artificial Neural Network framework a very useful tool for looking at nanofluid flows when it is affected by thermal radiation. The Artificial Neural Network model is really good, at this.

Table 1. Outcomes of ANN-BPLMT for all scenarios of BNF Model.

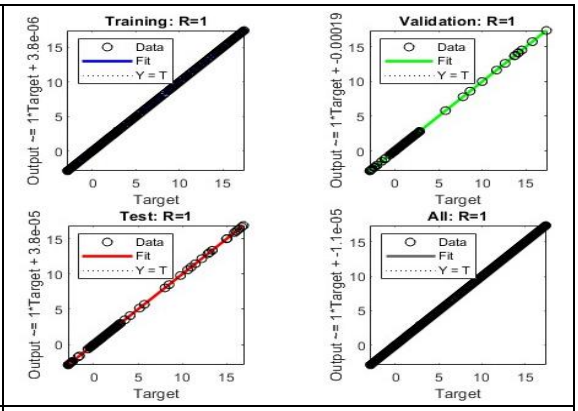
		Mean Square Error				Mu	Gradient		
Scenario	Case	Training	Validation	Testing	Performance	Parameter		Epochs	Time
S-1	1	1.9861E-04	1.6374E-04	2.7332E-04	1.99E-04	1.00E-06	9.61E-04	1000	08
	2	7.8787E-06	8.9377E-06	1.2357E-05	7.88E-06	1.00E-08	7.72E-04	1000	11
	3	1.4416E-05	2.3034E-05	1.3046E-05	1.44E-05	1.00E-06	5.75E-05	1000	08
	4	1.3201E-05	1.1464E-05	9.9572E-06	1.32E-05	1.00E-06	2.3E-04	1000	08
S-2	1	6.4324E-04	9.8522E-04	2.6831E-04	6.43E-04	1.00E-06	3.51E-04	1000	08
	2	1.3504E-05	9.9937E-06	1.2723E-05	1.35E-05	1.00E-06	7.62E-05	1000	10
	3	1.2903E-05	1.4104E-05	1.3706E-05	1.29E-05	1.00E-07	1.64E-04	1000	09
	4	6.8583E-06	9.1123E-06	5.3217E-06	6.86E-06	1.00E-07	4.81E-05	928	08
S-3	1	6.4324E-04	9.8522E-04	2.6831E-04	6.43E-04	1.00E-06	3.51E-04	1000	13
	2	1.4859E-05	1.2775E-05	1.7373E-05	1.49E-05	1.00E-06	1.08E-04	1000	09
	3	8.0988E-06	2.5831E-05	1.1244E-05	8.1E-06	1.00E-07	1.39E-04	1000	10
	4	4.4930E-06	4.9615E-06	5.1261E-06	4.49E-06	1.00E-07	9.71E-04	1000	10
S-4	1	5.4673E-06	6.2086E-06	8.3276E-06	5.47E-06	1.00E-07	1.65E-04	1000	14
	2	3.3072E-06	3.1690E-06	4.0770E-06	3.31E-06	1.00E-07	6.78E-04	1000	11
	3	2.5311E-04	1.2828E-04	1.6528E-04	2.53E-04	1.00E-06	9.76E-04	1000	11
	4	8.1300E-04	5.2593E-05	1.4785E-04	7.9E-04	1.00E-06	5.92E-04	38	01
S-5	1	5.1178E-06	4.8069E-06	7.2277E-06	5.12E-06	1.00E-08	3.99E-04	1000	14
	2	2.9751E-05	2.9516E-05	2.8259E-05	2.98E-05	1.00E-06	1.02E-04	1000	11
	3	9.8912E-05	1.0606E-04	1.0045E-04	9.85E-05	1.00E-07	7.23E-04	1000	03
	4	8.6105E-05	1.3033E-04	5.3011E-05	8.61E-05	1.00E-05	5.22E-04	1000	10
S-6	1	4.6083E-06	5.1876E-06	7.6082E-06	4.61E-06	1.00E-07	2.3.2E-04	1000	12
	2	1.3899E-05	1.2670E-05	1.7284E-05	1.39E-05	1.00E-06	1.22E-04	1000	08
	3	2.1233E-05	1.7767E-05	1.7909E-05	2.12E-05	1.00E-06	5.96E-05	1000	07
	4	5.6446E-06	8.9321E-06	7.1064E-06	5.64E-06	1.00E-06	2.13E-04	1000	06
S-7	1	3.3753E-04	4.1468E-04	8.2363E-04	3.33E-04	1.00E-05	4.11E-04	136	03
	2	6.7834E-06	6.6060E-06	6.6533E-06	6.78E-06	1.00E-07	1.79E-04	1000	05
	3	3.8742E-06	4.1092E-06	3.9481E-06	3.87E-06	1.00E-08	4.66E-04	1000	04
	4	7.3498E-05	8.3187E-05	8.5115E-05	7.35E-05	1.00E-05	1.64E-04	1000	04
S-8	1	1.9562E-06	2.7963E-06	3.5050E-06	1.96E-06	1.00E-07	9.15E-04	1000	06
	2	4.9489E-06	7.5623E-06	5.6315E-06	4.95E-06	1.00E-08	2.46E-04	1000	04
	3	1.8850E-05	1.7570E-05	2.0204E-05	1.89E-05	1.00E-07	1.83E-04	1000	04
	4	7.9932E-05	8.8666E-05	7.9485E-05	7.99E-05	1.00E-07	2.79E-04	1000	06

Results and Discussion:

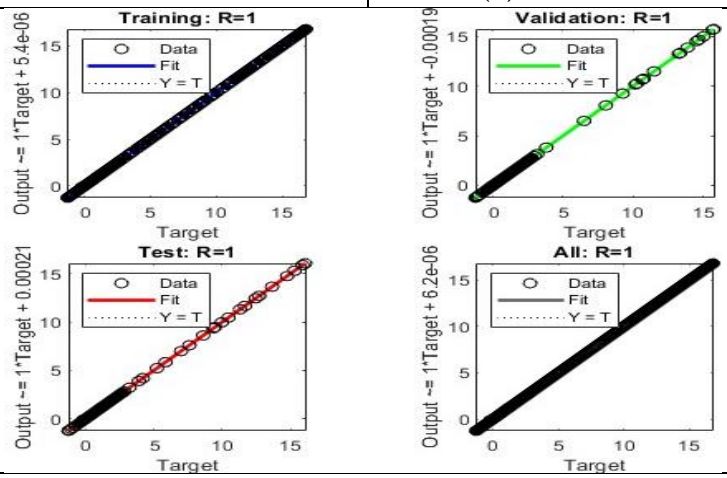
Table 1 presents the eight scenarios with all the 4 cases and the computational results are also presented in tables and graphs which demonstrate the accuracy and efficiency of the ANN model. The different scenarios and corresponding parameter variations considered in the present study for both velocity temperature profiles. These conditions are to investigate the effects of important physical parameters on the flow and heat transfer characteristics of the nanofluid system in a systematic manner. The graphical representations of the prediction framework can be found in Figure 4 sets (A) to (O) provided illustrations in the form of regression, transition state, performance validation, error histogram and fitness curves respectively. The correlation coefficient R, approaching unity statically as depicted in figures, signifies the optimal value for training, testing, and validation phases. Figure 5 illustrates the step-by-step procedure of the entire study.



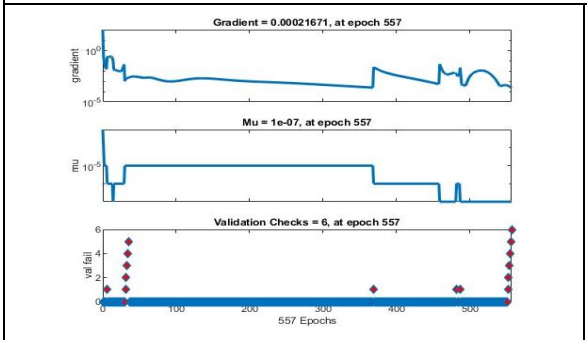
(A) Case-II of a/c for $\theta(\eta)$



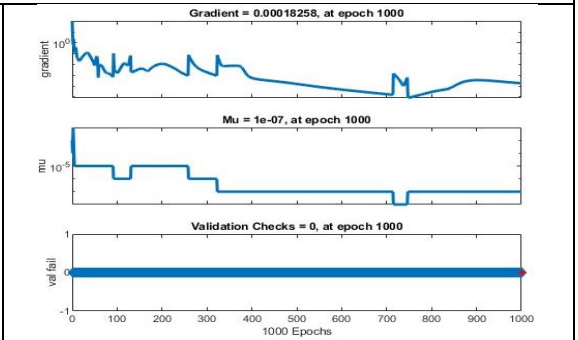
(B) Case-II of $\Pr$ for $\theta(\eta)$



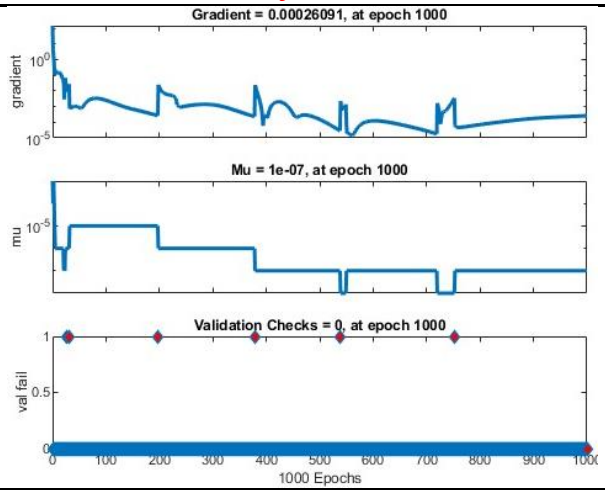
(C) Case-II of a/c for $f'(\eta)$



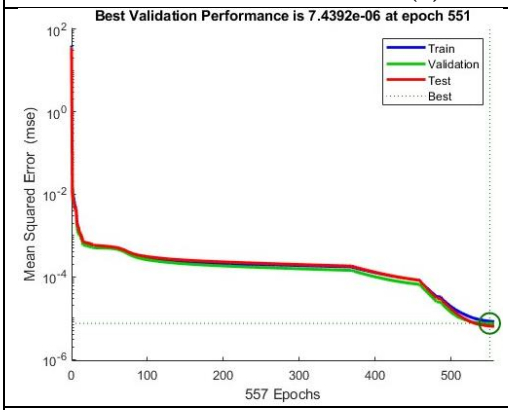
(D) Case-II of a/c for $\theta(\eta)$



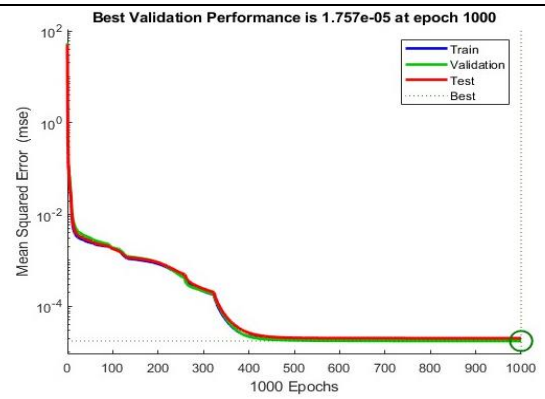
(E) Case-II of $\Pr$ for $\theta(\eta)$



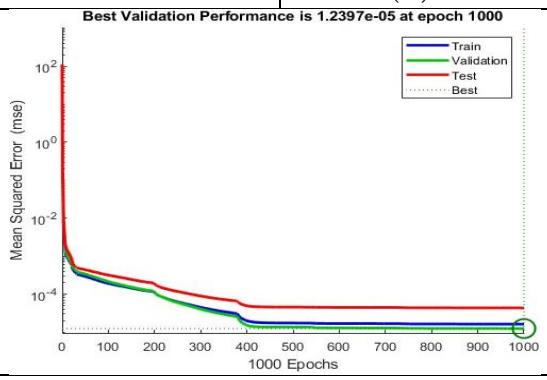
(F) Case-II of a/c for $f'(\eta)$



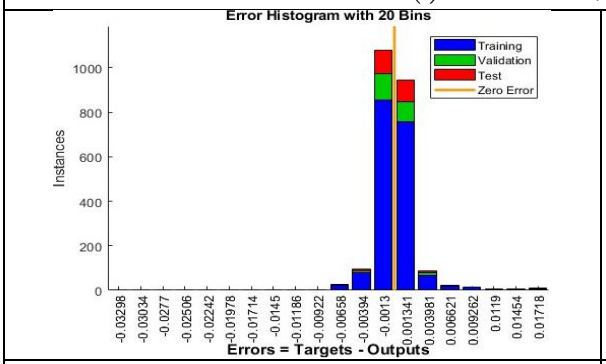
(G) Case-II of a/c for $\theta(\eta)$



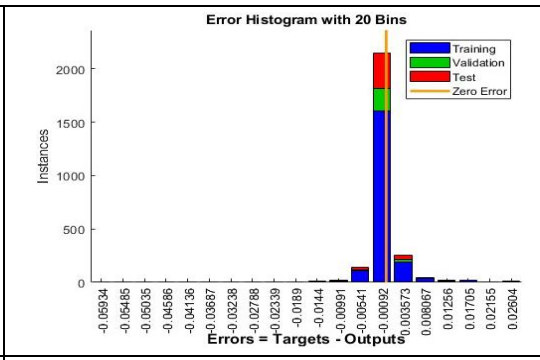
(H) Case-II of Pr for $\theta(\eta)$



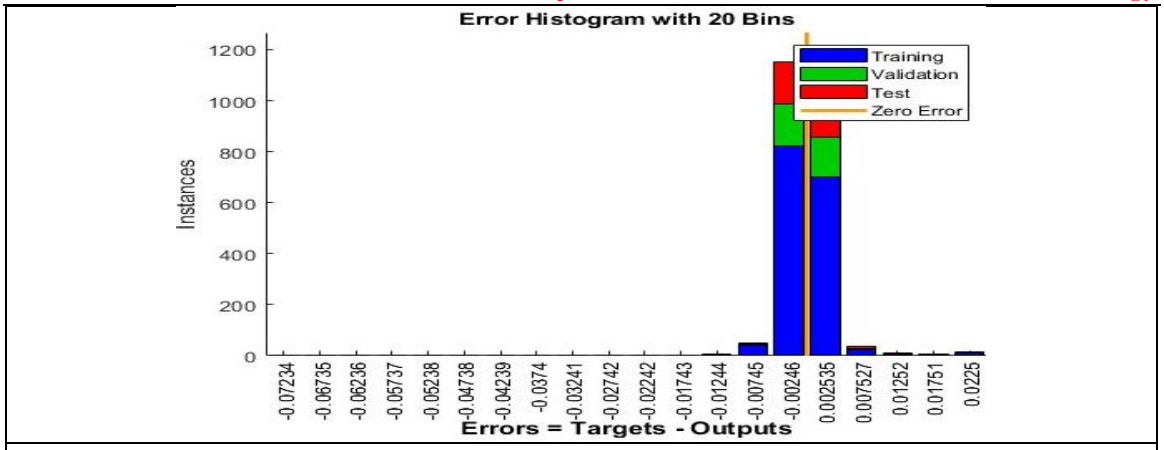
(I) Case-II of a/c for $f'(\eta)$



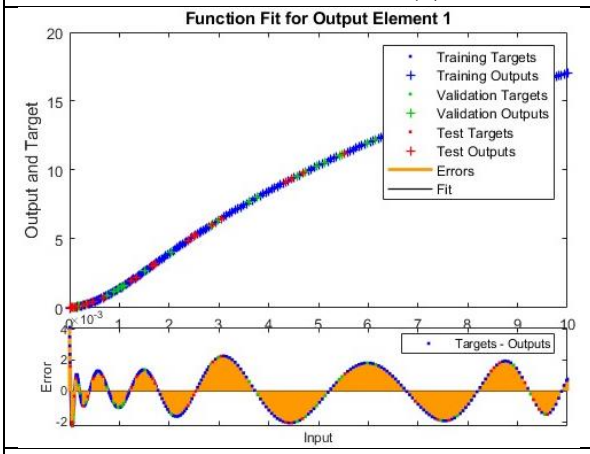
(J) Case-II of a/c for $\theta(\eta)$



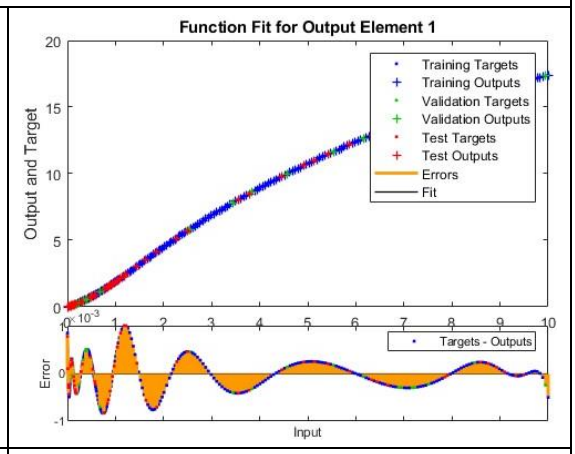
(K) Case-II of Pr for $\theta(\eta)$



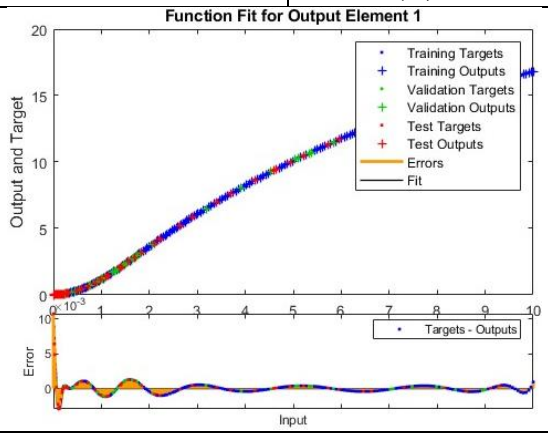
(L) Case-II of a/c for $f'(\eta)$



(M) Case-II of a/c for $\theta(\eta)$



(N) Case-II of Pr for $\theta(\eta)$



(O) Case-II of a/c for $f'(\eta)$

Figure 4. Step by step ANN Framework in form of errors

A very close agreement between predicted and actual concentration values is indicated by this plot and reliability of the ANN model is confirmed by small deviation for concentration prediction. The Levenberg–Marquardt algorithm predicts the velocity with great precision and negligible error with very low mean squared error (MSE). The developed ANN model learns the thermal behavior of Nanofluid as confirmed by the testing, validation, and training errors. The histogram shows that most prediction errors are concentrated near zero, indicating excellent prediction accuracy. This narrow error distribution is consistent with the very small MSE values reported in the numerical table. A symmetric distribution around zero is exhibited

by error histogram with very few large deviations. The accurate and unbiased temperature predictions are provided by ANN is confirmed by this graph. There is a rapid decrease in performance curve and after some time, reaches a minimum MSE, indicated by fast convergence of the training process. If there is no significant divergence between training and validation errors, it will indicate that overfitting has been successfully avoided. The ANN demonstrates efficient learning by reaching optimal validation performance within a limited number of epochs. The low performance value confirms accurate temperature prediction and excellent convergence. The predicted temperature values closely match the target data throughout the entire dataset. The excellent fitting capability and prediction accuracy of the trained ANN is demonstrated by target data. The fit plot shows that the target velocity values are closely followed by the ANN outputs. The velocity characteristics of the nano fluid are confirmed to be accurately captured by the network, as indicated by the nearly overlapping curves.

Model Figure 4. ((A)- (C)) illustrates the regression plots for the temperature and velocity profiles. The lowest performance value of 1.96×10^{-6}, obtained in Scenario S-VIII, Case I indicates that the predicted outputs almost coincide with the numerical solutions. The negligible prediction errors imply an excellent linear relationship between the predicted and target values, with regression coefficients approaching unity. A nearly linear correlation exists between the target and predicted temperature and velocity distributions. The ANN model's outstanding predictive consistency is demonstrated by the data points gathering around the regression line.

Framework set ((D)- (F)) demonstrates the ANN transition for the temperature and velocity profiles. A representative result is Scenario S-2, Case IV, where the performance reaches 6.86×10^{-6}, with a learning parameter of 1×10^{-7}, a gradient of 4.81×10^{-5}, and convergence after 928 epochs in 8 seconds. Compared with the remaining cases, this result indicates faster convergence with fewer epochs while maintaining high prediction accuracy. A fast convergence tendency, suggesting that fewer computational iterations are needed for the ANN to provide an exact result. This illustrates the built network predicts temperature and velocity characteristics computationally.

Design set ((G)- (I)) presents the ANN performance for the temperature and velocity profiles. Among all cases, Scenario S-7, Case I produces the best performance with training, validation, and testing MSE values of 3.5050×10^{-6}, 2.763×10^{-6}, and 3.5050×10^{-6} respectively. The overall performance value is 1.96×10^{-6}, the learning parameter is 1×10^{-7}, and the network converges after 1000 epochs within 6 seconds. These very small prediction errors prove the high accuracy and stability of the ANN in evaluating both temperature and velocity distributions.

Network of images ((J)- (L)) depicts a histogram of prediction errors for temperature and velocity profiles. In Scenario S-8 Case I, 3.5050×10^{-6}, the testing error is very small showing that most prediction errors are close, to zero. his narrow distribution proves that the trained ANN model is consistent and strong. A symmetric distribution of residual errors, suggesting that the ANN forecasts for temperature and velocity characteristics are impartial and very trustworthy.

System of set ((M)- (O)) shows the ANN fitting for the temperature and velocity profiles. The best fitting is achieved in Scenario S-8, Case I, where the overall performance value is 1.96×10^{-6}, with validation and testing errors of 2.7963×10^{-6}, and 3.5050×10^{-6}, respectively. These extremely small errors demonstrate that the ANN predictions almost overlap with the numerical solutions, confirming the high predictive capability of the developed model. The optional ANN model may effectively replace modern numerical simulations for quick

prediction of heat transfer behavior in nanofluids, as demonstrated by the strong agreement between the two datasets.

Conclusions:

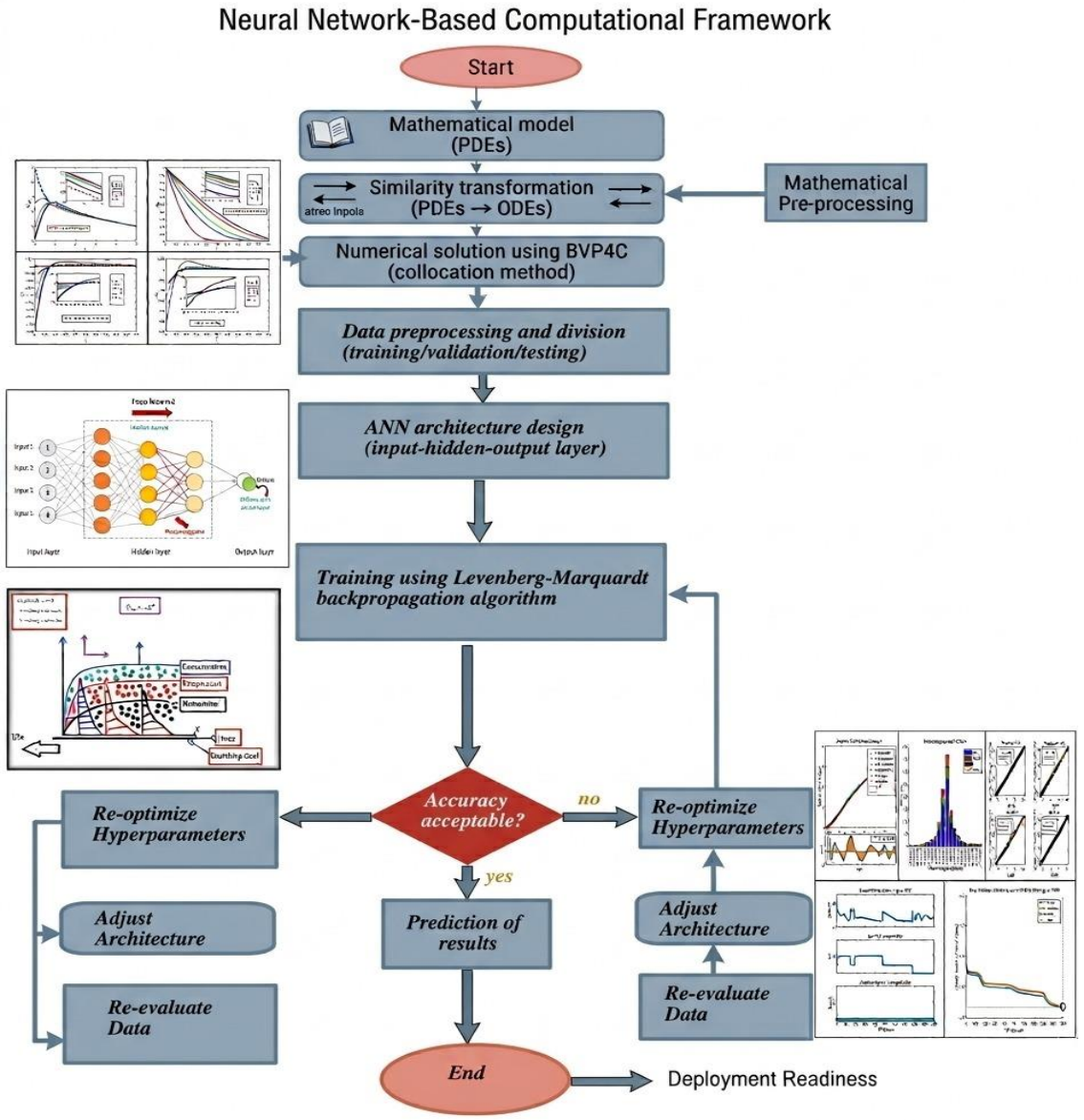


Figure 5. Flow Chart of Step-by- Step Work

In order to predict the concentration, temperature, and velocity profiles of nanofluid flow over a stretching sheet with changeable thermophysical properties, the current study effectively constructed an ANN model. By correctly identifying the nonlinear link between the governing parameters and the transport phenomena, the ANN model demonstrated outstanding prediction performance. It is also an addition, to traditional numerical techniques when it comes to analyzing difficult nanofluid flow and heat transfer issues. The Artificial Neural Network for Buongiorno nanofluid model with thermophysical variable properties has showed the following concluding remarks.

- The minimum ANN performance (MSE) of 1.46×10^{-6}, was attained in Scenario S-4, Case V, representative excellent prediction accuracy.
- Scenario S-8, Case I also produced a very low MSE of 1.96×10^{-6}, for the temperature and velocity profiles.

- Regression plots produced correlation coefficients ($R \approx 1$), confirming excellent contract between ANN calculations and numerical results.
- The transition plots showed steady convergence with adaptive learning parameters and small gradient values.
- Error histogram plots confirmed that calculation errors were concentrated near zero with no significant bias.
- ANN fitting curves carefully overlapped the numerical data, representative high fitting accuracy.
- Most training methods converged within 1000 epochs, while computation times ranged from 4 to 14 seconds.
- Very low proof and testing errors verified the strong generalization capability of the trained ANN model.
- The ANN positively captured the nonlinear behavior of concentration, temperature, and velocity distributions.
- The proposed ANN model significantly decreases computational effort compared with straight numerical techniques.
- The stable methodology can be extended to more complex nanofluid, hybrid nanofluid, and MHD heat transfer difficulties.

References:

[1] G. K. Ramesh, B. C. P. Kumara, B. J. Gireesha, and R. S. Reddy Gorla, "MHD Stagnation Point Flow of Nanofluid Towards a Stretching Surface with Variable Thickness and Thermal Radiation," *J. Nanofluids*, vol. 4, no. 2, pp. 247–253, Mar. 2015, doi: 10.1166/JON.2015.1144.

[2] A. Malvandi, F. Hedayati, and D. D. Ganji, "Nanofluid flow on the stagnation point of a permeable non-linearly stretching/shrinking sheet," *Alexandria Eng. J.*, vol. 57, no. 4, pp. 2199–2208, Dec. 2018, doi: 10.1016/J.AEJ.2017.08.010.

[3] M. Abdollahzadeh, A. A. Sedighi, and M. Esmailpour, "Stagnation point flow of nanofluids towards stretching sheet through a porous medium with heat generation," *J. Nanofluids*, vol. 7, no. 1, pp. 149–155, 2018, doi: 10.1166/jon.2018.1431.

[4] A. Ali, H. S. Khan, S. Saleem, and M. Hussan, "EMHD Nanofluid Flow with Radiation and Variable Heat Flux Effects along a Slandering Stretching Sheet," *Nanomater. 2022, Vol. 12, Page 3872*, vol. 12, no. 21, p. 3872, Nov. 2022, doi: 10.3390/NANO12213872.

[5] M. A. A. Hamad and M. Ferdows, "Similarity solution of boundary layer stagnation-point flow towards a heated porous stretching sheet saturated with a nanofluid with heat absorption/generation and suction/blowing: A Lie group analysis," *Commun. Nonlinear Sci. Numer. Simul.*, vol. 17, no. 1, pp. 132–140, Jan. 2012, doi: 10.1016/J.CNSNS.2011.02.024.

[6] J. Jeong, C. Li, Y. Kwon, J. Lee, S. H. Kim, and R. Yun, "Particle shape effect on the viscosity and thermal conductivity of ZnO nanofluids," *Int. J. Refrig.*, vol. 36, no. 8, pp. 2233–2241, Dec. 2013, doi: 10.1016/J.IJREFRIG.2013.07.024.

[7] M. Hemmat Esfe, S. Saedodin, and M. Mahmoodi, "Experimental studies on the convective heat transfer performance and thermophysical properties of MgO–water nanofluid under turbulent flow," *Exp. Therm. Fluid Sci.*, vol. 52, pp. 68–78, Jan. 2014, doi: 10.1016/J.EXPTHERMFLUSCI.2013.08.023.

[8] M. A. Z. Raja, A. Latif, M. Khalid, K. S. Nisar, and M. Shoaib, "Intelligent predictive networks for Cattaneo-Christov heat and mass transfer dissipated Williamson fluid through double stratification," *Case Stud. Therm. Eng.*, vol. 64, p. 105411, Dec. 2024, doi: 10.1016/J.CSITE.2024.105411.

[9] M. A. Z. Raja, A. Latif, M. Shamim, K. S. Nisar, and M. Shoaib, "Design of artificial neural network for buongiorno model with nanofluids flow through stretching sheet," *Case Stud. Therm. Eng.*, vol. 69, p. 106054, May 2025, doi: 10.1016/J.CSITE.2025.106054.

[10] M. A. Z. Raja, A. Latif, M. Shamim, K. S. Nisar, and M. Shoaib, "A stochastic numerical analysis for viscoelastic fluid traversing a permeable perpendicular surface," *Int. Commun. Heat Mass Transf.*, vol. 165, p. 108996, Jun. 2025, doi: 10.1016/J.ICHEATMASSTRANSFER.2025.108996.

[11] B. Alqahtani, Z. Mahmood, M. A. Alyami, A. M. Alotaibi, U. Khan, and A. M. Galal, "Heat and mass transfer analysis of MHD stagnation point flow of carbon nanotubes with convective stretching disk and viscous dissipation," *Adv. Mech. Eng.*, vol. 14, no. 10, Oct. 2022, doi: 10.1177/16878132221128390;WGROUP:STRING:PUBLICATION.

[12] A. Latif, S. Iftikhar, H. Ali, S. Sheraz Asghar, F. Pakistan, and A. S. S, "MatLab Bvp4c Technique to Compute Thermophoresis and Brownian Motion in Nanofluid Flow Over a Transient Stretching Sheet," *Int. J. Innov. Sci. Technol.*, vol. 7, no. 3, pp. 2171–2183, Sep. 2025, doi: 10.33411/IJIST/1554.

[13] H. Zargartalebi, M. Ghalambaz, A. Noghrehabadi, and A. Chamkha, "Stagnation-point heat transfer of nanofluids toward stretching sheets with variable thermo-physical properties," *Adv. Powder Technol.*, vol. 26, no. 3, pp. 819–829, May 2015, doi: 10.1016/J.APT.2015.02.008.

[14] M. Abd El-Aziz, "Effect of time-dependent chemical reaction on stagnation point flow and heat transfer over a stretching sheet in a nanofluid," *Phys. Scr.*, vol. 89, no. 8, p. 085205, Jul. 2014, doi: 10.1088/0031-8949/89/8/085205.

[15] W. A. Khan, O. D. Makinde, and Z. H. Khan, "Non-aligned MHD stagnation point flow of variable viscosity nanofluids past a stretching sheet with radiative heat," *Int. J. Heat Mass Transf.*, vol. 96, pp. 525–534, May 2016, doi: 10.1016/J.IJHEATMASSTRANSFER.2016.01.052.

[16] C. S. K. Raju, N. Sandeep, M. Jayachandra Babu, and J. V. Ramana Reddy, "Stagnation-Point Flow of a Ferrofluid Towards a Stretching Sheet," *J. Nanofluids*, vol. 5, pp. 245–252, 2016, [Online]. Available: https://www.ingentaconnect.com/contentone/asp/jon/2016/00000005/00000002/art00007?crawler=true&mimetype=application/pdf

[17] A. Hamid, Hashim, M. Khan, and A. Hafeez, "Unsteady stagnation-point flow of Williamson fluid generated by stretching/shrinking sheet with Ohmic heating," *Int. J. Heat Mass Transf.*, vol. 126, pp. 933–940, Nov. 2018, doi: 10.1016/J.IJHEATMASSTRANSFER.2018.05.076.

[18] M. Khan, T. Salahuddin, S. Ayub, M. Altanji, and S. R. Saydaxmetova, "Stagnation point flow of a heated stretching surface boundary layer with temperature dependent viscosity," *Chinese J. Phys.*, vol. 90, pp. 846–852, Aug. 2024, doi: 10.1016/J.CJPH.2024.06.009.

[19] T. Muhammad *et al.*, "Thermo-bioconvection in stagnation point flow of third-grade nanofluid towards a stretching cylinder involving motile microorganisms," *PhyS*, vol. 96, no. 3, p. 035208, Mar. 2021, doi: 10.1088/1402-4896/ABD441.

[20] A. Abbasi, W. Farooq, F. Mabood, and Z. Hussain, "Finite difference simulation for oblique stagnation point flow of viscous nanofluid towards a stretching cylinder," *Phys. Scr.*, vol. 96, no. 1, Jan. 2021, doi: 10.1088/1402-4896/ABC927.

[21] I. Khan *et al.*, "Design of Neural Network with Levenberg-Marquardt and Bayesian Regularization Backpropagation for Solving Pantograph Delay Differential Equations," *IEEE Access*, vol. 8, pp. 137918–137933, 2020, doi:

10.1109/ACCESS.2020.3011820.

[22] S. A. A. Shah, F. S. Alshammari, M. F. Malik, and S. Batool, "Numerical–ANN Framework for Thermal Analysis of MHD Water-Based Prandtl Nanofluid Flow over a Stretching Sheet Using Bvp4c," *Symmetry 2025, Vol. 17, Page 1347*, vol. 17, no. 8, p. 1347, Aug. 2025, doi: 10.3390/SYM17081347.

[23] H. Pourpasha, P. Farshad, and S. Zeinali Heris, "Modeling and optimization the effective parameters of nanofluid heat transfer performance using artificial neural network and genetic algorithm method," *Energy Reports*, vol. 7, pp. 8447–8464, Nov. 2021, doi: 10.1016/J.EGYR.2021.10.121.

[24] G. Fan *et al.*, "A well-trained artificial neural network (ANN) using the trainlm algorithm for predicting the rheological behavior of water – Ethylene glycol/WO3 – MWCNTs nanofluid," *Int. Commun. Heat Mass Transf.*, vol. 131, p. 105857, Feb. 2022, doi: 10.1016/J.ICHEATMASSTRANSFER.2021.105857.

[25] S. Liaqat, A. A. Alhashmi, I. H. Jaghdam, T. M. Alkhaldi, M. Abbas, and A. A. Darem, "Bayesian regularization optimization technique for hybrid nanofluid with Cattaneo Christov flux model using wax and sand nanoparticles," *Discov. Nano 2026 211*, vol. 21, no. 1, pp. 143-, Apr. 2026, doi: 10.1186/S11671-026-04531-8.

[26] I. Khan and M. W. Ahmed Khan, "Artificial neural networking for computational assessment of ternary hybrid nanofluid flow caused by a stretching sheet: implications of machine-learning approach," *Eng. Appl. Comput. Fluid Mech.*, vol. 18, no. 1, Dec. 2024, doi: 10.1080/19942060.2024.2411786.

Copyright © by authors and 50Sea. This work is licensed under Creative Commons Attribution 4.0 International License.